Title

Experimental analysis of the influence of microcapsule mass fraction on the thermal and rheological behavior of a PCM slurry

Authors

Mónica Delgado*, Ana Lázaro, Conchita Peñalosa, Belen Zalba

Aragón Institute for Engineering Research (I3A), Thermal Engineering and Energy Systems Group, University of Zaragoza

Agustín Betancourt Building, C/María de Luna 3, 50018 Zaragoza, Spain

Phone: (+34) 976761000 ext: 5258, Fax: (+34) 976762616

* Corresponding Author, monica@unizar.es

Email addresses: ana.lazaro@unizar.es (Ana Lázaro), conchita.penalosa@unizar.es (Conchita Peñalosa), bzalba@unizar.es (Belén Zalba).

Abstract

A microencapsulated PCM (Phase Change Material) slurry with three different PCM mass fractions (14, 20 and 30%) has been analyzed. The present study investigates the influence of the PCM microcapsule mass fraction on the thermal and rheological characterization. Specifically, the Enthalpy-Temperature curves, the Thermal Conductivity-Temperature curves and the Viscosity-Shear rate curves have been determined. In addition, the physical stability under thermo-mechanical cycles has also been studied, as well as the heat transfer phenomenon and the fluid mechanics. The results have shown an enhancement in the heat transfer phenomenon, the slurry with 20% PCM microcapsules being the best option for use as a heat transfer fluid. Rupture of the PCM microcapsules was only observed for the slurry with 30% PCM microcapsules, after being pumped during three weeks and having experienced 10000 solidification-melting cycles.

Keywords: Microencapsulated PCM slurry, Convective heat transfer, Thermal Energy Storage, Thermophysical properties, Rheological properties, Physical stability

Nomenclature

Bi biot number

f fraction of heat losses

h enthalpy (kJ/kg)

G' elastic module (Pa)

G'' loss module (Pa)

I current (A)

k multiplier fitting coefficient (s)

m exponent fitting coefficient (-)

$\dot{m}$ mass flow rate (kg/s)

$\dot{Q}$ heating power absorbed or transported by the fluid (W)

T temperature (ºC)

$\dot{W}$ pumping power (W)

ΔU voltage (V)

1-D one dimensional

Greek symbols

α convective heat transfer coefficient (W/(m^2·K))

$\dot{\gamma}$ shear rate (1/s)

η energy ratio

μ steady shear viscosity (Pa·s)

Subscripts

in inlet of the heat transfer section

m1 melting beginning

m2 melting complete

out outlet of the heat transfer section

0 low shear rates

∞ high shear rates

Abbreviation

COP Coefficient of Performance

mPCM Microencapsulated Phase Change Material

PCM Phase Change Material

RTO Operation Temperatures Range

1. Introduction

Thermal energy storage based on the use of solid-liquid phase change of materials (PCM) is of increasing practical interest. Such interest is motivated by the considerable thermal energy storage density per unit volume of PCM materials in a reduced temperature range, and also by the constant incorporation of new materials with very different properties and phase change temperature intervals. The interest in phase change materials is evident when considering

thermal energy storage systems with PCM which have been developed for different applications [1].

Recently, a new technique has been proposed for the use of phase change materials in thermal storage systems, heat exchangers and thermal control systems. This new technique consists of forming a two-phase fluid by combining a fluid such as water and a phase change material such as paraffin, resulting in a latent heat storage fluid. Inaba [2] has classified thermal fluids, describing their main characteristics and applications. These latent thermal fluids include the following five types: 1) ice slurries; 2) phase change material microemulsions; 3) microencapsulated PCM slurries; 4) clathrate hydrate PCM slurries and 5) shape-stabilized PCM slurries (ssPCM slurries). The present experimental study is focused on microencapsulated PCM slurries.

These new fluids offer many advantages and can be used either as thermal storage materials or heat transfer fluids [3] due to 1) their high storage capacity during phase change, 2) the possibility of using the same medium either to transport or to store energy, as these slurries are pumpable (thus reducing heat transfer losses), 3) heat transfer at an approximately constant temperature, 4) a high heat transfer rate due to the elevated ratio surface/volume, 5) lower pumping power, as a consequence of the reduction in mass flow due to the higher heat capacity, and 6) a better heat exchange than conventional heat transfer fluids, due to the decrease in fluid temperature as a consequence of the higher heat capacity. Furthermore, these novel fluids have a more advantageous thermal energy storage density than conventional systems of sensible heat storage in water, and can compete with macroencapsulated PCM tanks. Besides, the response time may be shorter using these PCM emulsions or mPCM slurries as storage material than with macroencapsulated PCM. The tanks will be simpler as there is no need to macroencapsulate, and conventional tanks can be used.

Huang et al. [4] listed the recommendable properties for a PCM slurry utilized in cold storage and distribution systems. Specifically, the phase transformation range should match the designed operating temperature range. There should be an absence of subcooling, a narrow phase temperature range, a high heat transfer rate, and a low pressure drop in pumping

systems. Besides, the slurry should be stable during long-term storage and have reversible freezing/melting cycles under thermal-mechanical loads.

Among the different applications that appear on literature, it is found the utilization of these PCM slurries as thermal storage materials and heat transfer fluids in chilled ceiling [5-6]. In the first work, their authors present the simulation results of a combined system of chilled ceiling and storage tank with a PCM slurry. This PCM slurry was cooled and stored in the tank during the night, which resulted in electricity peak shaving, taking advantage of the nocturnal tariff and of a higher COP of the machine due to operation during lower environmental temperatures. During working hours, the PCM slurry flowed from the tank to the chilled ceiling, melting the PCM and releasing the latent heat. In the work of Griffiths and Eames, they quantified the reduction of the mass flow flowing through a chilled ceiling in a room when working with a PCM slurry. The mass flow is reduced from 0.7 L/s down to 0.25 L/s. Furthermore it could absorb energy at a constant temperature, avoiding increments in the panel surface temperature when internal gains increased. Another well-known application was carried out at the Narita Airport in Tokyo by Shibutani [7]. The change of refrigerants duet to environmental reasons resulted in lower cooling power and the chiller was non-capable to absorb the demand peaks at specific times of the day. This problem was solved through the installation of a tank filled with a PCM slurry. Pollerber and Dötsch [8] also proposed the use of PCM emulsions for cooling supply networks, allowing for the reduction of the pumping power and pipe dimensions, with lower operation and investment costs.

Although there are numerous advantages in the use of PCM slurries, there is a lack of technical experience. The main issues encountered when using a thermal storage material are subcooling and the unstable processes presented by slurries. When using heat transfer fluids, a higher heat transfer rate compared to water is of interest but existing studies have not obtained clear conclusions.

Delgado et al. [9] presented a review of the different parameters influencing the objective magnitudes in PCM slurries. Specifically, the different effects that the mass fraction has on the heat transfer phenomenon are listed in a table. From this compilation, it was concluded that increasing the PCM mass fraction in suspension had two opposite effects. On the one hand,

this increase means a decrease in the Stefan number and therefore an improvement in the convective heat transfer coefficient. On the other hand, the increase also means an increase in the viscosity and a decrease in the thermal conductivity, resulting in a worse heat transfer phenomenon.

A previous work by the present authors described an experimental installation for studying the heat transfer phenomenon and fluid mechanics [10]. In this installation, a PCM slurry with a 10% PCM microcapsule mass fraction was analyzed, pending the analysis of the influence of higher PCM microcapsule mass fractions on the heat transfer and on the flow characteristics. The present study aims to complete this previous work and to include thermophysical and rheological characterization. The paper compiles and analyzes the results of heat transfer and fluid mechanics from a detailed methodology for a mPCM slurry with three different PCM microcapsule mass fractions: 14%, 20% and 30%, to analyze wich PCM microcapsule mass fraction is suitable to be used as heat transfer fluid. The thermophysical and rheological properties have been obtained and the measurement methodology in the case of working with PCM slurries described thoroughly. This characterization has allowed to understand the heat transfer process. Physical stability has also been analyzed. Table 1 compiles the different characteristics investigated in this paper, together with the experimental devices used for their characterization.

2. Materials and properties

The studied mPCM slurry consists of microcapsules of paraffin coated by a polymer and dispersed in water through detergents. The mass fraction of the PCM microcapsules in the three mPCM slurries is 14%, 20% and 30%, respectively. The particle size distribution is approximately 1-20 μm according to the manufacturer's data. This mPCM slurry has been purchased in the commercial market.

2.1 Enthalpy-temperature curves

The phase change temperature range and the phase change enthalpy as a function of the temperature were obtained using the T-history method [11-13]. When a material is characterized, the sample must be representative of the material in question. In this case, the

PCM slurry is composed of different substances. The volume of the sample should be at least a few cm^3 or more if possible [13] to ensure that it has the correct chemical and physical composition representative of the bulk material. For this reason, an installation using the T-history method was used to determine the Enthalpy-temperature curve during the phase change of the mPCM slurry. This method is based on comparing the temperature evolution of the PCM and a reference substance during cooling and heating against the ambient temperature of a chamber. This reference substance should be a substance with well-known thermal properties. The basic aspects of this methodology are:

- 1-D heat transfer in radial direction (samples contained in cylindrical containers)
- The systems formed by the container and the water (this is the reference substance) and the PCM respectively are lumped capacitance systems. The temperature of the substance and of the tube is uniform at all times (Bi<<1)
- Heat transfer from the containers of PCM and of the reference substance to the chamber air takes place by natural convection.

In this manner, the methodology proposed by Zhang et al. [11] consists of recording the ambient temperature and the temperature of the sample and of the reference substance, contained in identical containers. Once obtained the Temperature-Time curves of both substances, these data can be processed to estimate the Enthalpy-Temperature curves. Figure 1 shows the Enthalpy-Temperature curve for the melting and solidification of the mPCM slurries, obtained by the T-history method. The phase change temperature range of the mPCM slurry in the three cases was approximately 21-24ºC and the phase change enthalpy for this range was 15.3 kJ/kg, 21.1 kJ/kg and 28 kJ/kg for the 14%, 20% and 30% mPCM slurry, respectively. The phase change enthalpy is especially low in the slurry with a 14% mass fraction, since there is only a 14% PCM microcapasules. The remaining 86% would be formed by water and other substances. Furthermore each microcapsule is formed by the phase change material and by the polymeric shell, reducing the effective fraction of PCM in suspension. It is not available the core fraction for this material, however it is known that the core usually constitutes between 20 and 95% of the total mass [9]. For this reason, the phase change enthalpy is quite low with very low PCM microcapsule mass fractions and a sharp rise in the enthalpy is not noticeable, due to the

low content of PCM in the compound. Hysteresis and subcooling phenomena were not observed when comparing the solidification and melting curves.

2.2 Thermal conductivity-temperature curves

Thermal diffusivity measurements have been made with a Laser Flash device from Netzsch, model LFA 457 MicroFlash. The Laser Flash method was initially designed for measurements in solids, where the thickness of the sample is known, standards are not necessary and the property is measured in the transient response. This method is indirect, since the thermal conductivity property is obtained from the measurement of other properties, in this case the thermal diffusivity, the density and heat capacity values.

The density measurements have been obtained from the measurement of the sample mass using a Mettler Toledo precision balance (accuracy 1 mg) and from the volume measurement of the sample in a calibrated test-tube of 10 mL at room temperature (standard deviation: 0,021 mL). This value has been taken as a constant value in the temperature range of the test. For the heat capacity measurement, a differential scanning calorimeter (DSC) from Netzsch, model DSC 200 F3 Maia, has been used, with an accuracy of 1% in the heat capacity measurement.

For obtaining the thermal diffusivity, one of the sample surfaces was heated in a homogeneous manner using a laser pulse, where the voltage and transmission filter were controlled. Using this method, the heat absorbed in the surface is transferred through the sample and an increase in temperature is produced in the rear surface. This increase is measured over time from a liquid nitrogen-cooled InSb photocell. A mathematical model describes the temperature rise versus time signal, and this was fitted to the experimental data using a non-linear regression algorithm.

Few studies can be found in the literature that measure liquids with the Laser Flash method [14-16], and only one involves a PCM changing its phase, specifically $NaNO_3$ [17] .To measure the thermal diffusivity in liquids, a special sample holder is necessary to contain the mPCM slurries. The sample is introduced between two layers of a material whose properties are well-known. The thickness and distances between the two layers are also perfectly known. In this way, the material can be evaluated as a three-layer compound, where the unknown factor is the intermediate layer.

The presence of the sample holder for liquids may disturb the process of heat conduction during the transient heating of the sample. Coquard and Panel [16] analyzed the influence of different parameters or phenomena on the results of the liquids. These authors considered that all the materials of the sample holder were opaque to the infrared radiative heat. They ignored the natural convection in the samples, considering the heat transfer purely conductive. They also assumed the heat transfer of the external surfaces with the environment occurred by convection and radiation. Consequently, the total external heat transfer was considered as an only coefficient h.

To estimate the uncertainty, Coquard and Panel made a review of the parameters that may cause errors. They concluded that the correct determination of the sample thickness and a rigorous filling up of the sample holder were key parameters. An air fraction in the sample of about 1.25% meant errors up to 15.4%, since this air layer would work as a thermal barrier. They also observed that infrared radiation could not propagate in water. Thus the hypothesis of no radiative exchange did not mean an error when measurements were made in materials with a sufficient amount of water.

The sample holder for liquids supplied by Netzsch is made of Pt90Rh10, whose thermal conductivity is 38 W/(m·K). This is a very high value compared to the thermal conductivity of the liquids to be measured (in the range from 0.15 to 0.6 W/(m·K)). However, the sample holder from Netzsch provides a side space between the base and the lid. The thermal resistance of this air space is higher than the thermal resistance of the liquid to be measured, minimizing the heat transfer through the sample holder. The same phenomenon occurs with the upper contact. However, given that the joint is not under pressure, the thermal resistance is higher than the thermal resistance of the fluid. It can be said that the influence of the sample holder on the results has been minimized.

Additionally, the empty sample holder has been tested and the response was compared to the response with the sample holder filled with water. A comparison of the results of both tests is shown in figure 2. The response is much longer when the sample holder is empty. When selecting the time range for the software to make the calculation, it is important that the data acquisition time should be short to avoid the contribution of the sample holder.

Regarding the measurement of the thermal diffusivity during the phase change from solid to liquid, since this is a transient method there may be great changes in the thermal properties during the phase change. However, the mathematical model considers constant properties. It was thus decided to make the measurements in the single-phase states, solid and liquid.

There are few standards for liquids in comparison to solids. Therefore, three different liquids were measured prior to the tests whose thermal diffusivity or conductivity is known: distilled water, hexadecane and glycerin. These liquids have thermal diffusivity values within the range of mPCM slurries for the temperature ranges of the application of these fluids.

To measure solid samples with the Laser Flash equipment, a vacuum was first created and then an inert atmosphere of N_2. However, when this procedure was carried out for liquids, the vacuum and the pressure reduction in the equipment chamber caused the water to evaporate when reaching the vapor pressure. This was checked by weighing the sample before and after the vacuum. Finally, the vacuum was omitted and a longer time was given for the creation of the N2 atmosphere.

The external surfaces of the sample holder were coated with graphite to increase the amount of energy absorbed and to guarantee that all the parts of the sample had the same absorption. The temperature of the front surface can reach very high values, so it is important to know the upper limit of this temperature to avoid transition phases of the tested material. In the case of water, it is necessary to avoid evaporation.

From the previous study by Coquard and Panel [16], it was known that a complete filling up of the sample holder was crucial, as well as the correct determination of the thickness of the liquid sample. The sample thickness was obtained from the measurements of the thickness of the sample holder executed by a caliber. In order to guarantee the complete filling up of the sample holder, the volume of the liquid sample holder was calculated from the geometrical data and the amount of sample was controlled by a micropipette.

Taking all these considerations into account, thermal conductivity values were obtained for the three liquids tested: water, hexadecane and glycerin. The values are shown in figure 3. These values are the average value of five pulses executed both for thermal diffusivity and

279 temperature, together the standard deviation of these measurements. In the case of distilled
280 water, the results show a maximum error of 7.87% and for hexadecane 4.31%. In the case of
281 glycerin, higher errors were obtained, up to 15.38%. The reference values for water,
282 hexadecane and glycerin were taken from the following references, respectively [18-20].
283 Although due to the graph scale is not very perceptible, these obtained values show an
284 increasing monotonous variation with temperature.

285 The thermal diffusivity values were obtained from the three layer model provided by the
286 equipment software. Figure 4 shows the thermal conductivity values for the mPCM slurries with
287 PCM microcapsule mass fractions of 14%, 20% and 30%. The measurements taken at 20ºC are
288 not considered very reliable, since even a very small increase in the temperature due to the
289 laser pulse will cause the heat capacity to change abruptly (phase change region between 20
290 and 24ºC) and this methodology may be not valid given that the heat capacity is considered
291 constant in the calculation. So if the attention is paid to the values at 25 and at 30ºC, it can be
292 observed that thermal conductivity of PCM slurries increases slightly when temperature rises. It
293 must be pointed out that the increase of the PCM microcapsule mass fraction entails a
294 decrease of the thermal conductivity. This behavior was expected, as the thermal conductivity of
295 paraffin is lower than of the water. Specifically the slurry for the PCM microcapsule mass
296 fraction of 14, 20 and 30% have experienced a 24, 32 and 39% reduction in comparison to
297 water respectively at a temperature of 30ºC.

298 **2.3 Rheological characterization**

299 To complete the present study, the Viscosity-Shear rate curves have been obtained with a
300 control stress rheometer from TA Instruments, model AR-G2. There are several works in the
301 literature where Viscosity-Shear rate curves are presented. However, the authors do not
302 describe in great detail the procedure used to obtain them.

303 In this work, rotational tests have been carried out. These tests entail applying a torque (or
304 stress) and measuring the strain, in order to obtain viscosity values. The Viscosity-Shear rate
305 curves have been obtained through a shear sweep from 0.001 to 1000 s^{-1}. For this purpose, a
306 stress is applied to the sample. The measurement of viscosity is carried out when the material

has reached the state of steady flow. The stress is increased logarithmically and the process is repeated, providing the flow viscosity curve. For the definition of the steady flow state, a condition has been proposed that the variation of the stress for three consecutive points should be lower than 5%. When this condition is reached, it is considered that the steady flow state has been reached.

In the works found in the literature describing part of the measurement procedure, a cone tends to be used as the geometry [21-22]. However, in this case a stainless steel plate of 40 mm has been chosen because of the size of the PCM microcapsules in suspension. These PCM microcapsules have a diameter range from 1 to 20 μm, according to the manufacturer's data. It is important that in the rotational tests, the particles can flow without any problem. A gap (or the truncated gap in cones) must be 10 times higher than the size of the particles in suspension. For this reason the plate was chosen, where the gap can be controlled. In the rotational tests with the plate, there is no constant shear rate along the radius of the geometry (unlike the cone). Therefore, a correction (included in the software of the rheometer) must be applied.

It must be mentioned that this geometry allows the use of the "solvent trap" accessory. With this accessory, a saturated atmosphere of humidity is created, avoiding the drying of the sample. For the temperature control of the sample, a Peltier plate was used. The Peltier plate guarantees that the plate is at the set temperature. If the set temperature is much higher or much lower than the room temperature, temperature gradients in the sample will be able to take place. In this case, the Peltier plate is considered the appropriate temperature controller, since the temperatures of the test are temperatures close to the room temperature, and because the "solvent trap" accessory can be used with this configuration.

Before obtaining the viscosity measurements, a time sweep (oscillatory test) was done to study the possible drying of the sample, and to determine in this way the maximum time of the tests (to avoid this phenomenon and to avoid the obtaining of incorrect measurements). In the time sweep, the elastic (G') and the loss (G'') components of the mPCM slurry are measured over time for a set frequency and strain (within the viscoelastic region). The fact that the sample dries would cause an increase in the elastic component (G') and an increase in the loss component (G''), as the resulting sample would have a higher PCM mass fraction as the water evaporates.

336 The time sweep was done without the solvent trap (without a water-saturated atmosphere). As
337 the slurries are complex fluids, a pre-shear of 100 1/s was carried out for 1 minute in order to
338 completely destroy the structure of the sample. In this way, if during loading the sample
339 structure is partially broken, the sample would be completely broken. It was observed that to
340 recover the structure required at least 600 seconds and that from 1200 seconds the sample
341 starts to evaporate. This time (1200-600=600 seconds) is insufficient to carry out the test. When
342 the geometry rose, it was observed that the sample was dried at the edges. The visual results
343 agreed with the results obtained with the rheometer. For this reason, the use of the solvent trap
344 with water was necessary.

345 Regarding the Viscosity-Shear rate curves at 27ºC shown in figure 5, the curves for the slurries
346 with 14% and 20% PCM microcapsule mass fractions are very similar to each other. The slurry
347 with a 14% PCM microcapsule mass fraction has a viscosity approximately 5 times higher than
348 water, the 20% slurry 6 times higher and the 30% slurry 18 times higher. It is observed that
349 when increasing the shear rate, the viscosity decreases down to the Newtonian plateau, where
350 the viscosity remains constant. This shear-thinning behaviour has also been found in the
351 majority of the works in this field found in the literature [21-24]. Other works show a Newtonian
352 behaviour when working with PCM concentrations lower than 25% [25-26]. This shear thinning
353 behaviour can be explained through the spatial layout of the microcapsules in suspension.
354 When a slurry is stable and at rest, the particles are dispersed randomly in the continuous
355 phase. When the slurry is sheared, there is no cooperative motion between the microcapsules
356 so that these microcapsules move in the flow direction and therefore the viscosity is high.
357 However, when the slurry is sheared at high shear rates, the microcapsules start to move from
358 their random layout to a situation where they start to form layers. In this way, the average
359 distance between microcapsules decreases in the flow direction and increases in the direction
360 perpendicular to the flow. This change of the spatial layout makes the motion is much easier
361 and decreases the viscosity [27].

362 It is also observed for the slurry with 14% and 20% PCM microcapsule mass fractions that the
363 flow curve starts to increase at approximately 200 s^{-1}. Rotational tests with liquids of very low

viscosity at very high shear rates may cause secondary flows, increasing the apparent viscosity [27].

The "Best Viscosity-Shear rate" tool of the rheometer software was used, which provided the behaviour equation that relates the viscosity to the shear rate that best fits with the measured values. The equation that best predicts the shape of the flow curve for the three mPCM slurries is the Carreau model [28]. This model is defined according to Equation 1:

$$\frac{\mu - \mu_\infty}{\mu_0 - \mu_\infty} = \frac{1}{(1 + (k\dot{\gamma})^2)^{m/2}} \quad (1)$$

where μ_0 and μ_∞ refer to the asymptotic values of viscosity at very low and very high shear rates respectively, k is a constant parameter with the dimension of time and m is a dimensionless constant. Table 2 shows the values of these parameters.

3. Pressure drop and heat transfer analysis

To study both flow and heat transfer characteristics of these mPCM slurries (basically to measure the convective heat transfer under constant heat flux and the pressure drop flowing through a circular tube), a flow loop was designed and built. This installation appears in figure 6 with the label of each device. In order to obtain these convective coefficients, it is necessary to record the heat flux absorbed by the heat transfer section of the figure, the fluid temperature and the wall temperature at several locations along this tube. This experimental setup consists of a thermostatic bath where the mPCM slurry is prepared to the set temperature and pumped to the flow loop. The mass flow is controlled and measured respectively by control valves and by a Coriolis flow meter. In the heat transfer section, heating wires supply uniformly-distributed heat flux. Finally, the mPCM slurry returns to the thermostatic bath for cooling.

The heat transfer section consists of a 10 mm copper tube, 1.82 m in length. Eleven type T thermocouples measure the wall temperature along the circular tube and two Pt100 sensors measure the fluid temperature at the inlet and at the outlet of the heat transfer section. The temperatures of the fluid along the tube were calculated. Ten isolated nichrome wires, connected in parallel, were coiled around the copper tube to heat the section. These heating

390 wires were connected to the 230 V AC power supply through a phase angle electronic regulator,
391 which allows the heating power provided to the heat transfer section to be varied. The maximum
392 heating power was 3600 W. The heat flux provided to the heat transfer section must guarantee
393 complete phase change of the dispersed PCM, so that the difference between the inlet and the
394 outlet temperatures is noticeable and higher than the Pt100 uncertainty. The current and the
395 voltage were measured by an ammeter and a voltmeter, respectively. Heat losses were
396 minimal, approximately 3%, and therefore the heat transfer section was not thermally isolated.
397 The heat losses were taken into account during data processing. A pressure differential
398 transducer measures the pressure drop in the heat transfer section. All measured data were
399 recorded by a HP-34970A Data Logger. The error introduced by the datalogger is negligible
400 with regard to the other measurement devices.

401 A previous article of the authors gives more specific details of the devices about the main
402 characteristic of the equipments and their measurement range [10]. This work also explains the
403 validation process of the experimental setup. This validation was accomplished by testing the
404 setup with water and comparing the results with theoretical values. Pressure drop, heat flux and
405 wall temperature measurements were successfully validated. Some differences were observed
406 between the experimental wall temperatures and those obtained by the analytical solution. In
407 these cases, an empirical correction model was established. This empirical model of correction
408 corrects such deviations, obtaining in this way an average error in the measurement of the wall
409 temperature of 0.24ºC. In this manner, the uncertainty in the measurement of the internal forced
410 convective coefficient from the experimental installation (taking into account that it will be
411 different for each local position and that it will depend on the measurement conditions, is around
412 5-10%.

413 **3.1 First measurements**

414 Prior to the flow and heat transfer tests, the energy balance must be verified to guarantee that
415 microcapsules do not adhere to any part of the experimental installation, since non-stable and
416 non-homogeneous mPCM slurries can increase the danger of obstruction [29]. When
417 calculating the energy balance (Equation 2), thermal equilibrium between the microcapsules
418 and water is assumed.

$$(1 - f)\cdot\Delta U\cdot I = \dot{m}\cdot(h[T_{out}] - h[T_{in}]) \quad (2)$$

The verification tests were performed for different mass flows and heat fluxes. Figure 7 shows the Enthalpy-Temperature curve obtained through the energy balance equation (along with its fitting to a sigmoid curve) and its comparison with the Enthalpy-Temperature curve previously obtained with the T-history installation. If the curves for the three PCM microcapsule mass fractions are compared to their respective h-T curves obtained with the T-history installation, it can be observed that the curve for the 30% PCM microcapsule mass fraction moves slightly towards higher temperatures. In addition, this phenomenon is accentuated when increasing the mass flow. On the other hand, for the 14% PCM microcapsule mass fraction, the curve is displaced towards lower temperatures in comparison to the curve obtained with the T-history installation. For the 20% PCM microcapsule mass fraction, both curves are almost the same. Three possible causes are suggested for these differences.

Firstly, in view of the curve for the 30% PCM microcapsule mass fraction, it was thought that a fraction of the microcapsules was deposited in different components of the installation, since according to the curve obtained in the experimental installation, the enthalpy was lower for the same fluid temperature. In order to check this hypothesis, the components more susceptible to deposition were dismantled. However, no deposition was observed either in the elbows or in the valves. Having dismissed this conjecture, it was considered that the differences could arise from the experimental installation itself (possibly inappropriate for determining the h-T curves). The slurry temperature for each section shows a temperature profile and according to this methodology an average temperature values is taken. These differences could also arise from the hypothesis that the thermal equilibrium between the PCM microcapsules and the water was incorrect, since there might be a heat transfer process between the PCM particles and the water. Regarding this last approach, Diaconu [30] studied numerically this heat transfer phenomenon between PCM microcapsules and water. In his results, he observed that the water temperature and the microcapsule temperature were very close each other, due to the high surface of heat exchange. The bigger differences appeared during melting and solidification, causing a hysteresis phenomenon. This hysteresis was influenced by the capsule diameter and by the heat transfer coefficient between the PCM capsules and the water.

448 **3.2 Evaluation as a thermal storage and heat transfer fluid compared to water**

449 As in the previous study [10], the evaluation of the PCM slurry with different PCM microcapsule
450 mass fractions began with the measurement of the pressure drop in the heat transfer section.
451 Figure 8 shows that when the PCM microcapsule mass fraction is increased to 30%, the
452 pressure drop increases significantly, whereas an increase in the PCM microcapsule mass
453 fraction from 14% to 20% hardly had any appreciable effect on the pressure drop. These results
454 correspond with the previous viscosity measurements. The slurry with a 14% PCM
455 microcapsule mass fraction and the slurry with a 20% PCM microcapsule mass fraction showed
456 a similar viscosity, while the viscosity of the slurry with a 30% PCM microcapsule mass fraction
457 was three times higher. From these pressure drop values and the phase change enthalpy, the
458 transported Thermal Energy vs. Pumping power compared to water could be evaluated. The
459 following energy ratio of improvement was defined (Equation 3) for this comparison:

460 $$\eta = \frac{\left(\frac{\dot{Q}_{mPCMslurry}}{\dot{W}_{mPCMslurry}}\right)}{\left(\frac{\dot{Q}_{water}}{\dot{W}_{water}}\right)} \quad (3)$$

461 Figure 9 shows this ratio obtained for different average fluid velocities while figure 10 shows the
462 Pumping power vs. Transported thermal energy ratio. It can be seen in figure 9 that if the PCM
463 microcapsule mass fraction is increased from 14 to 20%, the velocity from which the energy
464 ratio of improvement is equal to 1 decreases. In contrast, increasing the PCM microcapsule
465 mass fraction to 30% led to in an increase in this velocity, a consequence of the sharp increase
466 in the pressure drop observed in figure 8. In this case, for velocities lower than 1 m/s the
467 negative effect of the increase in the viscosity with the mass fraction is greater than the
468 improvement of the thermal energy that can be transported in comparison to water for the same
469 velocity. In figure 10, it is observed that for the same transported thermal energy, the pumping
470 power decreases in comparison to water.

471 To analyze the heat transfer characteristics, the mass flow and the heating power of the heat
472 transfer section were varied and the wall temperatures were measured. The tests were carried

473 out under the boundary condition of constant heat flux, the heat transfer section was a fully
474 hydrodynamic developed section and the flow was laminar, with mass flows from 20 to 50 kg/h.
475 The correction model was applied to the measured wall temperatures, and these values were
476 then compared to the calculated values for the case of water (obtained through Kays correlation
477 [31]). Dependence of the mass flow and the operation temperature range on the decrease in the
478 wall temperature was also studied. As in the previous paper, the same parameter, “operation
479 temperature range” was defined for the analysis, according to Equation 4. This parameter
480 shows if the phase change is in accordance with the heat transfer section. A parameter equal to
481 1 would mean that the mPCM slurry starts melting just as it enters the heat transfer section, and
482 leaves the heat transfer section only when the PCM microcapsules are completely melted. A
483 parameter under 1 would mean that the PCM microcapsules did not completely melt in the heat
484 transfer section, and a parameter above 1 means that both liquid and phase change regions
485 coexist in the heat transfer section. The parameter was defined taking into account the phase
486 change and liquid regions, attributing in this way different phenomena to each region.

487 Operation temperatures range $[RTO] = \frac{h[T_{out}] - h[T_{m1}]}{h[T_{m2}] - h[T_{m1}]}$ (4)

488 From the measurement of the wall temperature, the convective coefficients were obtained for
489 the laminar region. The results showed a significant decrease in the wall temperature compared
490 to water for the three different PCM microcapsule mass fractions, resulting in a better cooling
491 performance. This decrease in the wall temperature was higher when the “operation
492 temperature range” was higher. In the case of the heat transfer coefficients by convection, the
493 α_x-x curve for the slurry with PCM microcapsule mass fractions of 14 and 30% for the mass flow
494 of 50 kg/h was very close to the curve for water. The slurry with a mass fraction of 20% showed
495 better results. In spite of there being almost no improvement in the convective heat transfer
496 coefficient for the mass fractions of 14% and 30%, the wall temperature is lower in comparison
497 to water due to the decrease in the temperature of the mPCM slurry, as a consequence of its
498 higher heat capacity.

499 The tests were planned so that the *RTO* tested for the slurry with the 30% PCM microcapsule
500 mass fraction was the same as that for the tests with the slurries with 14% and 20% PCM

501 microcapsule mass fractions (*RTO*=0.75 and *RTO*=1.1), always calculated according to the
502 Enthalpy-Temperature curve obtained with the T-history installation. However, in the analysis of
503 the test results the phenomenon explained in section 3.1 was observed. The h-T curve obtained
504 from the energy balance was displaced for the slurry with the 30% PCM microcapsule mass
505 fraction. In this way, the outlet temperature of the fluid was determined with the *RTO* value, the
506 inlet temperature of the fluid and the values of enthalpy from the T-history curves. The heat flux
507 was controlled to reach this outlet temperature. In this manner the *RTO* parameter took the
508 values 0.68 and 0.89 when calculated from the h-T curves obtained through the energy balance
509 (whereas for the slurry with 14% and 20% PCM microcapsule mass fraction, the *RTO* was 0.75
510 and 1.1). In other words, the phase change was not completed in either of the two tests.

511 Figures 11 and 12 show the average decrease in the wall temperature (in Celsius scale) and
512 the average increase in the convective heat transfer coefficient with regard to the water for the
513 three PCM microcapsule mass fractions of 14%, 20% and 30%.

514 It can be observed that when increasing the PCM microcapsule mass fraction up to 30%, the
515 decrease in the wall temperature and the increase in the convective heat transfer coefficient are
516 lower than for the slurry with the 20% PCM microcapsule mass fraction but slightly higher than
517 that with the 14% PCM microcapsule mass fraction. The decrease in the wall temperature for
518 the 30% mass fraction compared to the 20% mass fraction is around 10% for the mass flow of
519 20 kg/h and around 38% for the mass flow of 50 kg/h. This decrease may be lower than that
520 with the 20% PCM microcapsule mass fraction because the RTO parameter for this case is
521 slightly lower, as a consequence of the *h-T* curve being slightly displaced with the temperature.

522 As mentioned in the previous paper [10], it is observed that when the “operation temperature
523 range” parameter fits with the phase change temperatures (*RTO*=1 or higher), the higher is the
524 decrease in the wall temperature. It is also observed in this case that higher mass flow or higher
525 velocities lead to a lesser improvement in the convective heat transfer coefficient. This can be
526 explained by the patterns of the thermally developing flow. At higher mass flow rates, the length
527 of the thermally developing region is greater. This means that for a given position, the fraction of
528 melted PCM microcapsules in that section is lower, resulting in a worse heat transfer from the
529 wall to the core region. This phenomenon would also occur at higher PCM mass fractions.

530 The decrease in the improvement of the heat transfer coefficient by convection when the PCM
531 microcapsule mass fraction increases from 20 to 30% is around 30% for the mass flow of 20
532 kg/h, and around 70% for the mass flow of 50 kg/h. This reduction may also be due to the
533 noticeable viscosity increase, as observed in figure 5, decreasing the degree of turbulence and
534 therefore worsening the heat transfer phenomenon. Another cause could be the lower effective
535 phase change enthalpy, since the *h*-*T* curve is displaced and the phase change is not
536 completed. The decrease in thermal conductivity deteriorates the heat transfer to the core
537 region of the flow. In this case the decrease in the thermal conductivity when the PCM
538 microcapsule mass fraction increases from 20 to 30% is around 10%, and around 40% lower
539 than water.

540 In view of these results, it can be stated that the slurry with a 20% PCM microcapsule mass
541 fraction is the most effective slurry regarding the heat transfer by convection, and taking into
542 account that for the slurry with a 30% PCM microcapsule mass fraction, a lower fraction of PCM
543 was melted.

544 **4. Physical stability**

545 During the tests with the slurry with a 30% PCM microcapsule mass fraction, the thermostatic
546 bath and pump were turned off during one day, stopping the flow of the slurry through the
547 installation loop. Without agitation, the PCM microcapsules in suspension separated from the
548 water and caused the clogging of one of the balanced valves. These samples were analyzed
549 with a microscope.

550 To study a possible rupture of the PCM microcapsules in suspension, samples of the slurries
551 were observed with a Philips XL30 environmental SEM (Scanning Electronic Microscope) after
552 being thermally cycled (melting and solidification cycles) and pumped. Preparation of the
553 sample is unnecessary for environmental SEMs and samples with water content can be
554 observed. This is possible because with the environmental SEM, there is a gas in the chamber
555 of the sample enabling the examination of samples which would be difficult to observe in a
556 conventional SEM for different reasons (for example, they are not conductive, they are not
557 compatible with the high vacuum of a conventional SEM, or they need difficult preparation

steps). When the gas present in the chamber is water vapour, then wet samples can be observed, even samples in solutions without the necessity of previous preparation. In addition to saving time and preparation material, the use of other devices, that may give a non-real observation of the sample, is not necessary.

Figure 13 shows a sample of the non-thermal-mechanical cycled slurry. The shape of the microcapsules is spherical, although certain cavities can be observed on the surface. The sample with a 30% PCM microcapsule mass fraction after undergoing thermal and mechanical cycles in the experimental installation during three weeks (having experienced approximately 10000 solidification-melting cycles) is shown in figure 14. The joins between the PCM microcapsules can be seen. To dismiss a possible optical effect resulting from the opacity of water to electrons, the sample was dehydrated during the observation, decreasing the pressure in the microscope chamber. Even with a pressure of 2 Torr, the effect appeared. Therefore, the fact that the microcapsules join each other as a consequence of their possible rupture can be confirmed. The sample with a 20% PCM microcapsule mass fraction but having undergone thermal-mechanical cycles during two weeks was also observed (having experienced approximately 7000 solidification-melting cycles). Its image was very similar to the non-cycled sample shown in figure 13. In this case, the microcapsules had not broken. It is possible that in the case of the sample with a 30% PCM microcapsule mass fraction, the rupture and subsequent joining of microcapsules to each other has caused the Enthalpy-Temperature to be displaced, because of the higher effective particle diameter. This decreases the heat transfer area and may cause hysteresis.

At the beginning, this analysis of the possible rupture of the PCM microcapsules was not considered in the frame of this work, so the number of thermo-mechanical cycles had not been set and it depended on the period of time of the tests. The best option to establish a correct comparison between the different samples had been subject to the different slurries at a same number of cycles. However this microscopy analysis was considered when analyzing the slurry with 30% PCM microcapsule mass fraction, due to the blockage of the installation. When this fact happened, the other slurries with lower PCM microcapsule mass fraction had been already tested. It is expected that with higher PCM microcapsules mass fraction, there is more contact

587 and friction among them and the rupture may take place more easily. It is evident that prior to
588 their use in a specific application, their stability should be studied for the predicted number of
589 cycles in the useful life of the system.

590 It is expected that with higher PCM microcapsules mass fraction, easier the rupture as more
591 contact and friction among them may take place

592 **5. Results compilation**

593 Table 3 shows the results compilation together with the main conclusions and findings of this
594 work.

595 **6. Conclusions**

596 A PCM slurry with three different mass fractions (14%, 20% and 30%) has been characterized.
597 Specifically, the Enthalpy-temperatures have been obtained. The methodology for obtaining
598 measurements of thermal diffusivity using Laser Flash equipment has been fully described. The
599 geometrical determination of the sample holder and its correct filling are crucial for obtaining
600 appropriate measurements. In the same manner, the methodology for obtaining the Viscosity-
601 Shear rate curves using a control stress rheometer has been described. The flow curves for the
602 three slurries are fitted to the Carreau model.
603
604 In the evaluation of the paraffin slurry as a new heat transfer fluid compared to water, it has
605 been observed that when increasing the mass fraction from 14% to 20%, the velocity from
606 which the $(\dot{Q}_{slurry}/\dot{W}_{slurry})/(\dot{Q}_{water}/\dot{W}_{water})$ ratio is higher than 1 decreases. However, when the
607 mass fraction was increased to 30%, this velocity rose as the viscosity increased sharply.
608
609 With regard to the heat transfer phenomenon, the convective heat transfer coefficient for the
610 three mass fractions represented an improvement in comparison to water. The slurry with the
611 20% mass fraction gave the best results, for the conditions of heat flux and velocity analyzed in
612 the frame of this work. If the attention is paid to the transported thermal energy in relation to the
613 pumping power, the slurry with 30% PCM microcapsule mass fraction would be the best option.
614 However the improvement of the slurry with the 30% PCM mass fraction was less than that with

615 the 20% mass fraction regarding the internal convective heat transfer phenomenon in the
616 analyzed range, probably as a consequence of an incomplete phase change, an increase in the
617 viscosity and a decrease in the thermal conductivity.
618
619 The slurries were observed with an environmental SEM after the pumping (thermal and
620 mechanical loads). In the case of the slurry with 30% PCM microcapsules, the rupture of the
621 microcapsules together with their subsequent joining together was observed after three weeks
622 of pumping (having experienced approximately 10000 solidification-melting cycles). When the
623 experimental process was stopped and the slurry was at rest, the same slurry blocked the
624 control valve. However, the microparticles in the slurry with 20% mass fraction were not
625 ruptured after having been pumped during two weeks (approximately 7000 solidification-melting
626 cycles).
627
628 It can be concluded that these slurries may be a suitable heat transfer and storage fluid.
629 However, before any technical application, the obtaining of more resistant microcapsules should
630 be studied.

631 **7. Acknowledgements**

632 The authors would like to thank the Spanish government for partially funding this work within the
633 framework of research projects (MICINN-FEDER): ENE2008-06687-CO2/CON, ENE2011-
634 28269-C03-01 and ENE2011-22722. Mónica Delgado is especially grateful to the Vice
635 Deanship for Research of the University of Zaragoza for her grant.

636 **8. References**

637 [1] B. Zalba, J.M. Marín, L.F. Cabeza, H. Mehling, Review on thermal energy storage with
638 phase change: materials, heat transfer analysis and applications, Appl. Therm. Eng. 23 (3)
639 (2003) 251-283.

640 [2] H. Inaba, New challenge in advanced thermal energy transportation using functionally
641 thermal fluids, Int. J. Therm. Sci. 39 (9-11) (2000) 991-1003.

642 [3] L. Royon, G. Guiffant, Forced convection heat transfer with slurry of phase change material
643 in circular ducts: A phenomenological approach, Energy Convers. Manag. 49 (5) (2008) 928-
644 932.

645 [4] L. Huang, M. Petermann, C. Doetsch, Evaluation of paraffin/water emulsion as a phase
646 change slurry for cooling applications, Energy 34 (9) (2009) 1145-1155.

647 [5] X. Wang, J. Niu, Performance of cooled-ceiling operating with MPCM slurry, Energy
648 Convers. Manag. 50 (3) (2009) 583-591.

649 [6] P.W. Griffiths, P.C. Eames, Performance of chilled ceiling panels using phase change
650 material slurries as the heat transport medium, Appl. Therm. Eng. 27 (10) (2007) 1756-1760.

651 [7] S. Shibutani, PCM-microcapsule slurry thermal storage system for cooling in Narita Airport,
652 3rd Experts meeting and Workshop of IEA, Annex 17, Tokyo (Japan), (2002).

653 [8] C. Pollerberg, C. Dötsch, Phase changing slurries in cooling and cold supply networks, 10th
654 International Symposium on District Heating and Cooling, Section 8A, 13, Hannover (Germany),
655 (2006).

656 [9] M. Delgado, A. Lázaro, J. Mazo, B. Zalba, Review on phase change material emulsions and
657 microencapsulated phase change material slurries: Materials, heat transfer studies and
658 applications, Renew. Sustain. Energy Rev. 16 (1) (2012) 253-273.

659 [10] M. Delgado, A. Lázaro, J. Mazo, J.M. Marín, B. Zalba, Experimental analysis of a
660 microencapsulated PCM slurry as thermal storage system and as heat transfer fluid in laminar
661 flow, Appl. Therm. Eng. 36 (2012) 370-377.

662 [11] Y. Zhang, Y. Jiang, Y. Jiang, A simple method, the T-history method, of determining the
663 heat of fusion, specific heat and thermal conductivity of phase-change materials, Meas. Sci.
664 Technol. 10 (3) (1999) 201-205.

665 [12] J.M. Marín, B. Zalba, L.F. Cabeza, H. Mehling, Determination of enthalpy-temperature
666 curves of phase change materials with the T-history method – improvement to temperatura
667 dependent properties, Meas. Sci. Technol. 14 (2) (2003) 184-189.

668 [13] A. Lázaro, E. Günther, H. Mehling, S. Hiebler, J.M. Marín, B. Zalba, Verification of a T-
669 history installation to measure enthalpy versus temperature curves of phase change materials,
670 Meas. Sci. Technol. 17 (8) (2006) 2168-2174.

671 [14] W.Q. Jin, T. Nagashima, S. Yoda, X.A. Liang, Z.L. Pan, Thermal difussivity measurements
672 of $Li_2B_4O_7$ and $KNbO_3$ solution by Laser Flash method, Chin. Phys. Lett. 19 (4) (2002) 569-71.

673 [15] J. Blumm, A. Lindemann, S. Min, Thermal characterization of liquids and pastes using the
674 flash technique, Thermochim. Acta 455 (1-2) (2007) 26-29.

675 [16] R. Coquard, B. Panel, Adaptation of the FLASH method to the measurement of the thermal
676 conductivity of liquids or pasty materials, Int. J. Therm. Sci. 48 (4) (2009) 747-760.

677 [17] T. Bauer, D. Laing, U. Kröner, R. Tamme, Sodium nitrate for high temperature latent heat
678 storage, The 11th International Conference on Thermal Energy Storage-Effstock, Lecture
679 number 4, Stockholm (Sweden) (2009).

680 [18] S.A. Klein, Engineering Equation Solver (2012) Academic Commercial V9.215.

681 [19] G.K. Mukhamedzyanov, A.G. Usmanov, A.A. Tarzimanov, Determinations of the thermal
682 conductivity of liquid saturated hydrocarbons. Izv Vyssh Ucheb Zaved Neft' I Gaz 6 (9) (1963)
683 75-79.

684 [20] R.H. Perry, D.W. Green, Perry's Chemical Engineers' Handbook, Mc Graw Hill, Sidney,
685 Australia, 1997.

686 [21] L. Huang, C. Doetsch, C. Pollerberg, Low temperature paraffin phase change emulsions,
687 Int. J. Refrig. 33 (8) (2010) 1583-1589.

688 [22] L. Royon, P. Perrot, G. Guiffant, S. Fraoua, Physical properties and thermorheological
689 behaviour of a dispersion having cold latent heat-storage material, Energy Convers. Manag. 39
690 (15) (1998) 1529-1535.

691 [23] W. Lu, S.A. Tassou, Experimental study of the thermal characteristics of phase change
692 slurries for active cooling, Appl. Energy 91 (1) (2012) 366-374.

693 [24] B. Chen, X. Wang, R. Zeng, Y. Zhang, X. Wang, J. Niu, Y. Li, H. Di, An experimental study
694 of convective heat transfer with microencapsulated phase change material suspension: Laminar
695 flow in a circular tube under constant heat flux, Exp. Therm. Fluid Sci. 32 (8) (2008) 1638-1646.

696 [25] X. Wang, J. Niu, Y. Li, X. Wang, B. Chen, R. Zeng, Q. Song, Y. Zhang, Flow and heat
697 transfer behaviors of phase change material slurries in a horizontal circular tube, Int. J. Heat
698 and Mass Transf. 50 (13-14) (2007) 2480-2491.

699 [26] G.H. Zhang, C.Y. Zhao, Thermal and rheological properties of microencapsulated phase
700 change materials, Renew. Energy 36 (11) (2011) 2959-2966.

701 [27] H.A. Barnes, A handbook of elementary rheology, Institute of Non-Newtonian Fluid
702 Mechanics. University of Wales, Aberystwyth, United Kingdom, 2000.

703 [28] J.P. Carreau, Rheological Equations from Molecular Network Theories, Trans. Soc. Rheol.
704 16 (1) (1972) 99-127.

705 [29] S. Gschwander, P. Schossig, Phase Change Slurries as heat transfer and storage fluids for
706 cooling applications, The 10th International Conference on Thermal Energy Storage-Ecostock,
707 Lecture number 55, New Jersey (USA), 2006.

708 [30] B.M. Diaconu, Transient thermal response of a PCS heat storage system, Energy Build. 41
709 (2) (2009) 212-219.

710 [31] W.M. Kays, Numerical Solutions for Laminar-Flow Heat Transfer in Circular Tubes, Trans.
711 ASME 77 (1955) 1265-1272.

712 **Figure captions**

739 **Table captions**
740

744

745

746

747

748

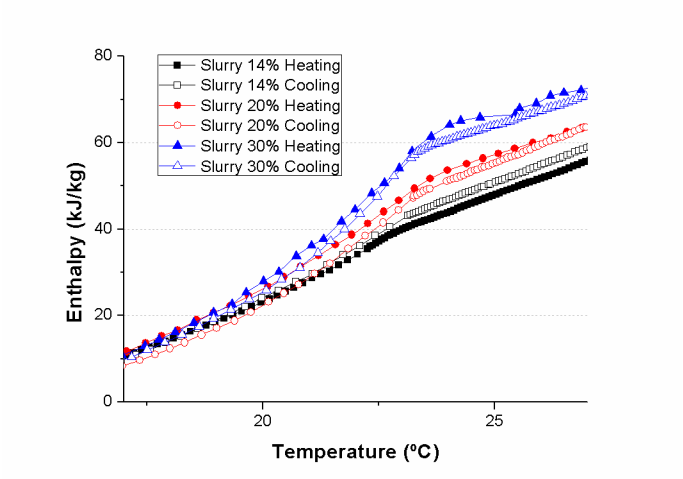

749

750 Figure 1.

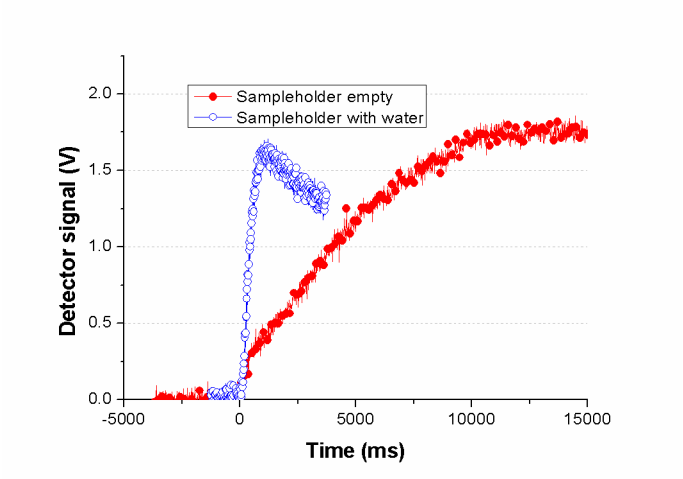

751

752 Figure 2.

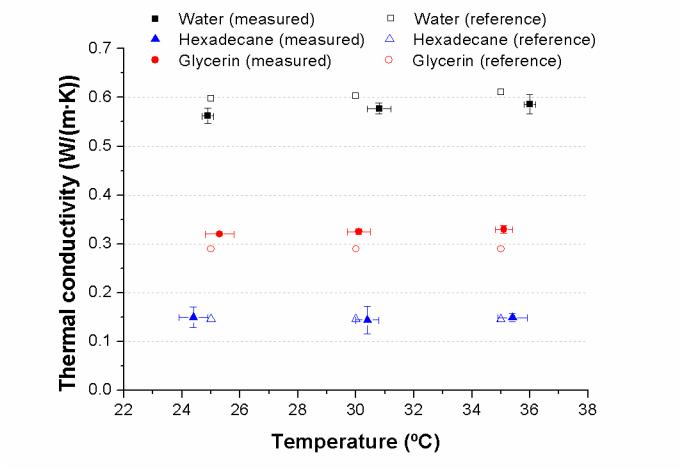

753

754 Figure 3.

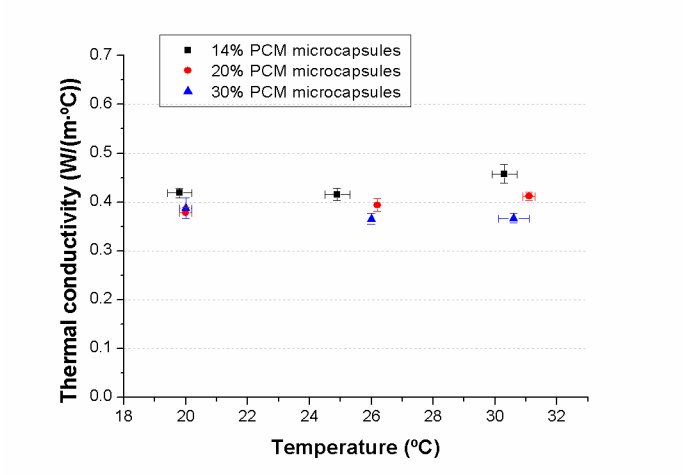

755

756 Figure 4.

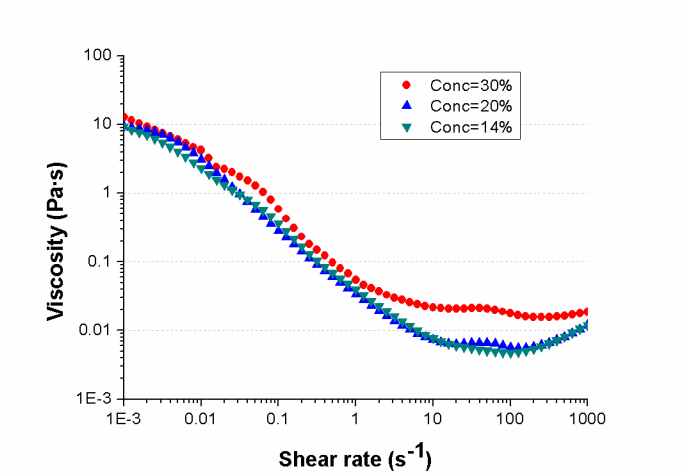

757

758 Figure 5.

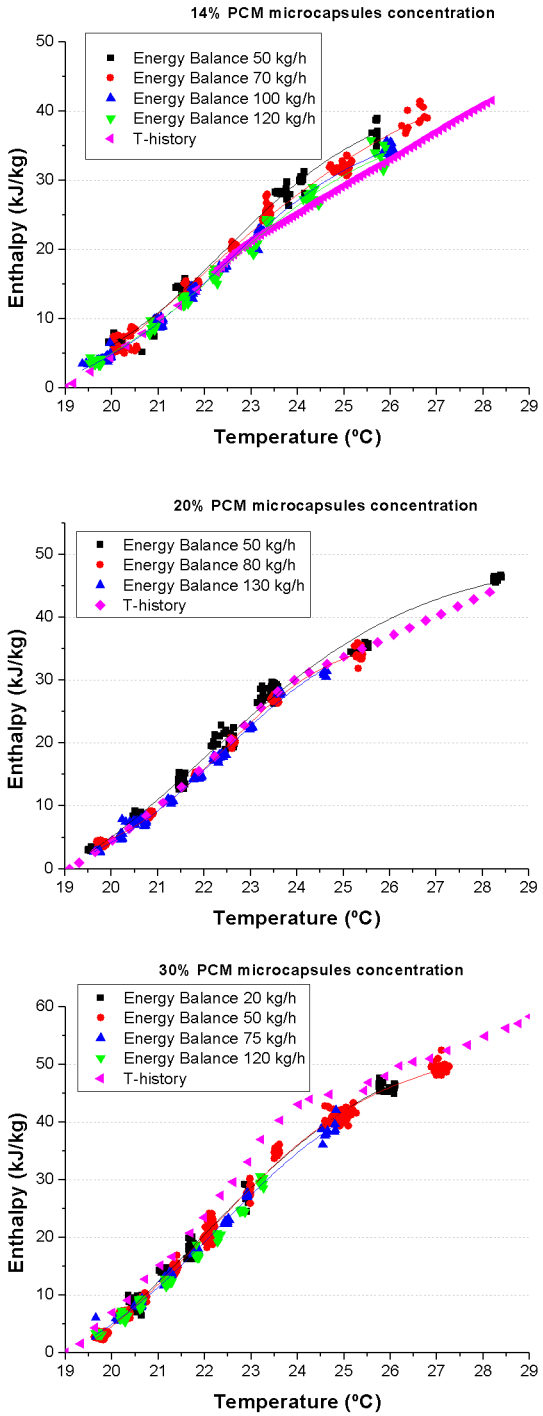

759

760 Figure 6.

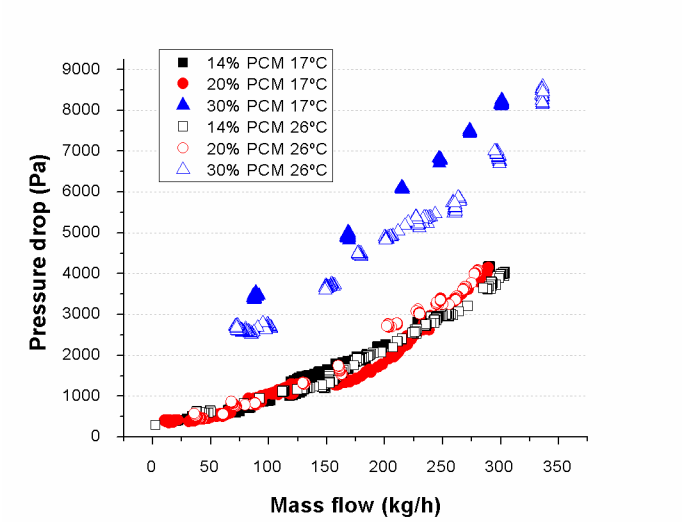

761

762 Figure 7.

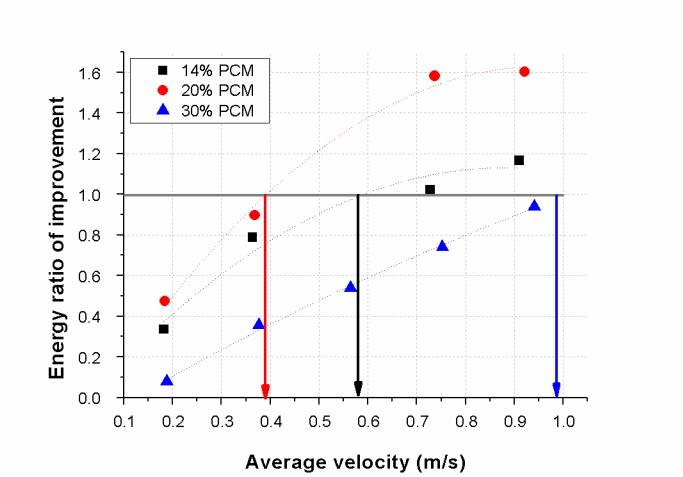

763

764 Figure 8.

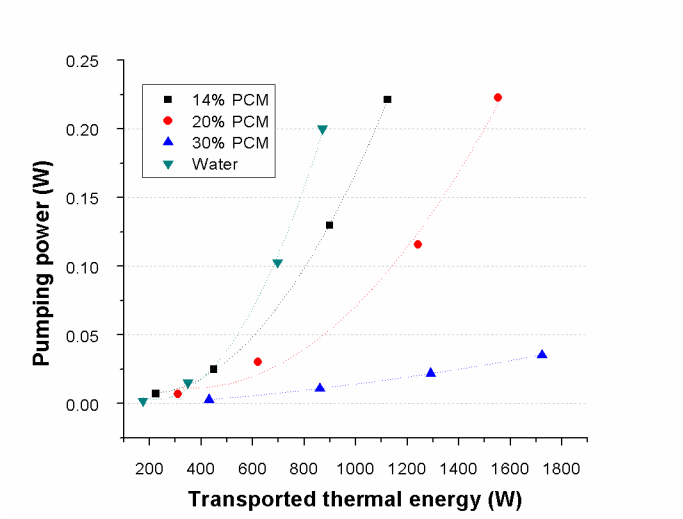

765

766 Figure 9.

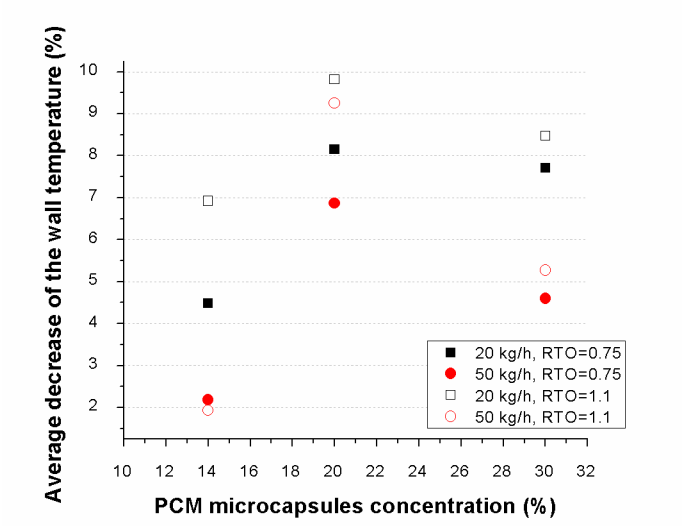

767

768 Figure 10.

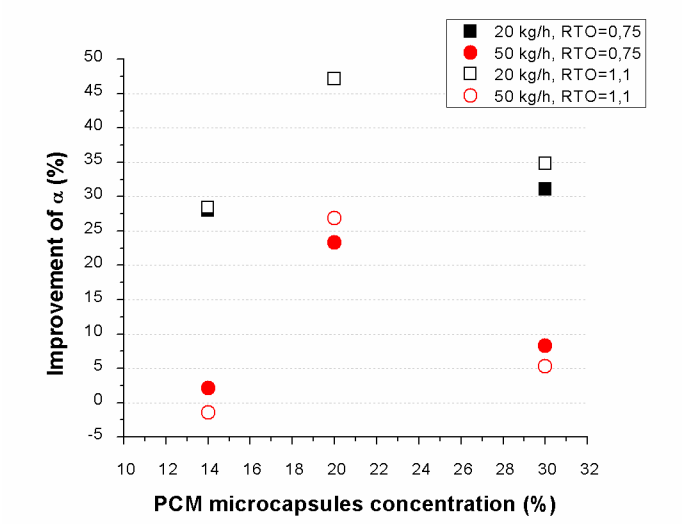

769

770 Figure 11.

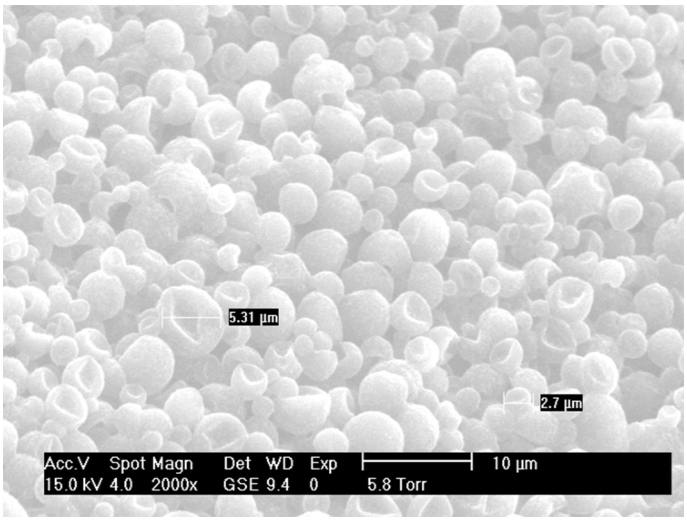

771

772 Figure 12.

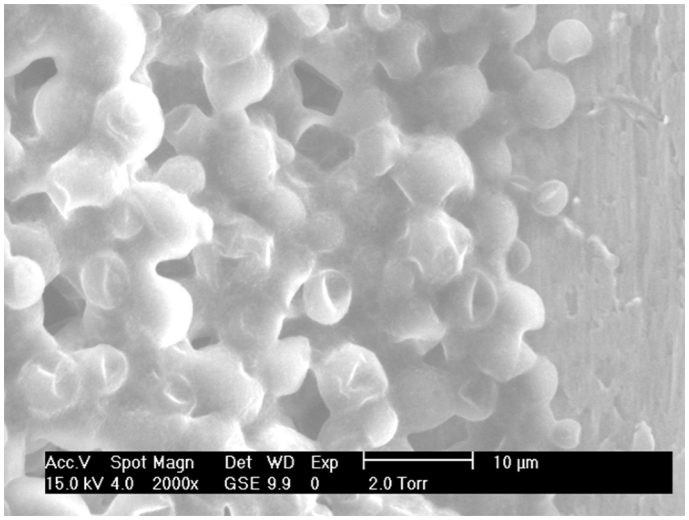

773

774 Figure 13.

775

Table 1. Compilation table of the characteristics analyzed in the experimental work.

	Characteristic to analyze	Equipment / method	Section
Properties	Enthalpy-Temperature curves	T-history method	2.1
	Thermal conductivity-Temperature curves	Laser Flash method, DSC	2.2
	Viscosity-Shear rate curves	Control stress rheometer	2.3
Fluid mechanics	Pressure drop	Experimental installation built for that purpose	3.2
Heat transfer	Heat transfer (forced convective heat transfer)	Experimental installation built for that purpose	3.2
Physical stability	Physical stability under thermo-mechanical loads	Environmental SEM	4

776

Table 2. Parameters according to the Carreau model [22].

PCM microcapsules concentration	η_0 (Pa·s)	η_∞ (Pa·s)	k (s)	m
14%	13.80	$4.89 \cdot 10^{-3}$	288.80	1.02
20%	10.88	$6.45 \cdot 10^{-3}$	315.40	1.06
30%	6.45	$18.32 \cdot 10^{-3}$	82.05	1.03

777